Interactions between Dendrimers and Charged Probe Molecules. 1. Theoretical Methods for Simulating Proton and Metal Ion Binding to Symmetric Polydentate Ligands

Li Sun*,† and Richard M. Crooks*,‡

Department of Chemistry, Texas A&M University, P.O. Box 30012, College Station, Texas 77842-3012

Received: January 18, 2002; In Final Form: April 2, 2002

Binding of protons and metal ions to dendrimers is investigated using a multishell model, in which concentric binding sites are approximated by continuous and uniformly charged shells. The electrostatic interactions among the shells are assumed to be the sole source of site-to-site interactions, and an analytical formula for the total interaction energy, which includes Coulomb screening from mobile electrolyte ions, has been derived. The formula permits numerical simulation of proton and metal-ion binding equilibria using two computational methods. The first method is a statistical approach in which the partition function is simplified by a mean-field approximation. The second method is derived by considering ion binding as a surface adsorption problem, and the resulting binding isotherm is a Frumkin isotherm. In most cases, the two methods give nearly the same results, but the isotherm method requires much less computation time. Proton binding as a function of pH for an individual shell follows a trend very similar to that for the overall averaged binding. Selective protonation of alternating shells, as observed for a previously described Ising model, is not observed in this study; instead, proton binding becomes increasingly weak as one moves from an outer shell toward the center of the dendrimer.

Introduction

Understanding the interactions between dendrimers and various probe molecules is important not only for optimizing existing applications of dendrimers but also for expanding the role of dendrimers in new applications. Existing applications that rely on controlled dendrimer−probe interactions include extraction of metal ions or organic molecules into the dendrimer interior, catalysis by dendrimer-encapsulated nanoparticles, and controlled loading or release of drug molecules from dendrimer hosts.[1−6]

Binding of small probe molecules to a polymer is often difficult to model theoretically because (i) a polymer has many degrees of freedom and therefore can assume numerous configurations, (ii) several modes of probe binding may exist, making it difficult to enumerate all configurations, and (iii) more than one probe can bind to a single polymer, so probe-to-probe interactions must be considered. However, Borkovec and Koper (B&K) have shown recently that despite the aforementioned difficulties, useful simulation results can be obtained for a particular simple binding problem: namely, the protonation of amine-containing dendrimers.[7,8] Their model, referred to as the "Ising model",[9] approximates proton−proton interactions by considering only localized electrostatic repulsions, such as those between nearest neighbors. Good results have been obtained from this model for linear as well as dendritic polyamines. Since a statistical method is used to implement the Ising model, it requires evaluating a partition function that contains many Boltzmann factors corresponding to all possible proton binding configurations. As the number of binding sites in a dendrimer increases, partition function calculation becomes more and more difficult because of rapid increase in computation time. In B&K's Ising model where only nearest neighbor interactions are considered, this difficulty can be overcome by using a recursive renormalization procedure.[7] However, it is not clear if the procedure is applicable to more complicated cases such as when next-nearest interactions are included or when additional binding moieties such as metal ions are considered.

In contrast, we adopted a shell-like dendrimer model to estimate site-to-site interactions. Dendrimer binding sites are grouped into concentric spherical shells, and each shell has a continuous and uniform charge distribution. The main advantage of this shell geometry is that an analytical expression for the total interaction energy can be obtained even when the Coulomb screening of mobile ions is included.

We have employed two methods for calculating binding properties of a shell dendrimer model. In the first method, we simplify partition function calculation by using a mean-field approximation reported earlier.[9,10] In the second method, we have considered dendrimer protonation from a slightly different perspective. Instead of considering the whole dendrimer structure, which inevitably runs into the problem of statistically evaluating numerous terms in a partition function, we focused our attention only on one individual binding site. This approach yields a binding isotherm that is similar in form to the Frumkin adsorption isotherm.[11] Using the isotherm approach to study polymeric binding properties is not new, and Tanford has detailed this subject in his famous monograph.[12] The isotherm method contains many approximations, but in some cases it gives nearly the same results as those from the mean-field statistical method. In addition, it requires much less computation than any statistical method discussed so far because it does not require partition function calculations. Decreasing the amount of computation is critical for extending a theory to a wider range of problems. For example, we are able to calculate the binding behavior of a metal ion to a dendrimer molecule whereas this

* To whom correspondence should be directed.
† Voice: 979-845-1595. Fax: 979-845-1399. E-mail: lisun@mail.chem.tamu.edu.
‡ Voice: 979-845-5629; fax: 979-845-1399; e-mail: crooks@tamu.edu.

10.1021/jp020189w CCC: $22.00
Published on Web 05/15/2002

is almost computationally prohibitive for methods based on statistical partition.

Results and Discussions

(1) Conventional or Macroscopic Approach to Metal−Ligand Binding Equilibria. For a polymeric and polydentate ligand L (electric charge is omitted here for simplicity and generality), its binding equilibria can be understood if all the equilibrium constants, often known as stability constants, are known.[13] The stability constant for species $M_kOH_lH_hL$ is

$$\beta(k, l, h) = \frac{[M_kOH_lH_hL]}{[M]^k[H]^{h-l}[L]} \qquad (k \geq 0, l \geq 0, h \geq 0) \quad (1.1)$$

The quantities in [ ] are concentrations, and they should be replaced with activities at high ionic strengths. As a first approximation, we will ignore the activity coefficients. k, l, and h can be thought of as the *binding numbers* for M, OH, and H, respectively. Note that OH binds to a ligand only through a metal ion already coordinated with the ligand. The hydroxyl concentration [OH] does not appear in (1.1) because it is related to proton concentration [H] by

$$\beta_w = [H][OH] = 10^{-13.78} \qquad (\text{at } 25\ ^\circ\text{C}) \quad (1.2)$$

where β_w, the autodissociation constant of water, has been absorbed into $\beta(k,l,h)$ implicitly.[13]

Using these stability constants, we can write three sets of material balance equations:

$$f_L = L_0 - \alpha_L^{-1}[L] = 0 \quad (1.3)$$

$$f_M = M_0 - [M] - \bar{k}L_0 = 0 \quad (1.4)$$

$$f_H = H_0 - B_0 - [H] + \beta_w[H]^{-1} - (\bar{h} - \bar{l})L_0 = 0 \quad (1.5)$$

where L_0, M_0, H_0, and B_0 are the total concentrations for L, M, H (strong acid added initially), and OH (strong base added initially), respectively, α_L is the fraction of the free ligand, and $\bar{k}$, $\bar{l}$, and $\bar{h}$ are the average binding number per ligand molecule for M, OH, and H, respectively. These variables are given by

$$\alpha_L = \frac{[L]}{L_0} = \left(\sum_{klh} \beta(k,l,h)[M]^k[H]^{h-l}\right)^{-1} \quad (1.6)$$

$$\bar{k} = \alpha_L \sum_{klh} k\beta(k,l,h)[M]^k[H]^{h-l} \quad (1.7)$$

$$\bar{l} = \alpha_L \sum_{klh} l\beta(k,l,h)[M]^k[H]^{h-l} \quad (1.8)$$

$$\bar{h} = \alpha_L \sum_{klh} h\beta(k,l,h)[M]^k[H]^{h-l} \quad (1.9)$$

It is clear that if all the $\beta(k,l,h)$ are known, then [M] and [H], or pM and pH, can be solved using (1.4) and (1.5). Searching solutions digitally in a two-dimensional parameter space defined by [M] and [H] is relatively easy because both f_M and f_H decrease monotonically as [M] or [H] increases. Searching stops when both f_M and f_H are zero.

A widely accepted method for determining stability constants is potentiometric pH titration.[13] In this method, L_0, M_0, and H_0 are known to a very high precision, and pH is measured continuously as B_0 is gradually increased by titrating a strong base into a sample solution. A complete set of $\beta(k,l,h)$ are guessed initially, and the pH, calculated using the aforementioned digital method, is compared with experimentally measured pH value. The sum of squared errors for all titration points (χ^2) is minimized through iterations to refine the initial guesses for $\beta(k,l,h)$. Although this method works very well for simple polydentate ligands, it failed completely for dendrimers since the number of possible $\beta(k,l,h)$ is large, and an iterative calculation for refining $\beta(k,l,h)$ is too slow to be practically useful. Even if this method is successful, it is still not very informative because the connection between the macroscopic stability constants and the structures (geometrical as well as chemical) of dendrimers is not obvious. In contrast, such a connection arises naturally in a statistical method.

(2) Statistical Approach to Metal−Ligand Binding Equilibria. Accurate statistical solutions to equilibrium problems can be obtained if all possible microstates are included in partition function calculations.[14] The partition function P is simply the sum of the Boltzmann factors for all microstates:

$$P = \sum_m \exp\left(-\frac{\mu_m}{k_BT}\right) = \sum_m \exp(-\beta_T\mu_m) \quad (2.1)$$

where T is the absolute temperature, k_B is the Boltzmann constant, β_T is the inverse of thermal energy, and μ_m is the binding free energy of microstate m with respect to a reference microstate (often chosen to be the state of a free ligand L).

To obtain more specific results, we make the following assumptions about the ligand which is either a poly(amidoamine) (PAMAM) or a poly(propylene imine) (PPI) dendrimer. First, each amine functional group can be taken to form four types of sites: vacancy site, H binding site, M binding site, or MOH binding site. In this study, we assume further that each metal center can bind a maximum of one OH group. This restriction can be removed but it will make partition function calculation slightly more complicated. Second, M and H bind competitively; thus, there is no binding site where both M and H coexist. In addition, one H binds only one amine group whereas one M binds γ_M coordinating amines. If the maximum binding number for H is h_0, then competitive binding implies that the maximum binding number for M or MOH will be k_0, and

$$h_0 = \gamma_M k_0 \quad (2.2)$$

With the above assumptions, the binding free energy for a particular microstate becomes

$$\mu_m = \mu^o(k,l,h) + \Delta\mu_m \quad (2.3)$$

where

$$\mu^o(k,l,h) = (k-l)\mu_M^o + l\mu_{MOH}^o + h\mu_H^o \quad (2.4)$$

$$\Delta\mu_m = \frac{1}{2}\left(\sum_s^{k-l}\Delta\mu_M^s + \sum_s^{l}\Delta\mu_{MOH}^s + \sum_s^{h}\Delta\mu_H^s\right) \quad (2.5)$$

Here, s is a binding-site index, and μ_M^o, μ_{MOH}^o, and μ_H^o are the intrinsic binding free energies at the sites designated in the subscript. An intrinsic binding energy, or the free energy measured when only one binding site per dendrimer molecule is occupied, can be estimated from the stability constant of a structurally similar ligand containing only one binding site.[9] For example,

$$\exp(-\beta_T \mu^o_H) = \beta_H[H] = 10^{pK_H - pH} \tag{2.6}$$

where β_H is the intrinsic stability constant for the H binding site and K_H its intrinsic acid dissociation constant. Similarly,

$$\exp(-\beta_T \mu^o_M) = \beta_M[M] \tag{2.7}$$

$$\exp(-\beta_T \mu^o_{MOH}) = \beta_{MOH}[M][H]^{-1} \tag{2.8}$$

If more than one binding sites are occupied, the binding energy per site will deviate from the intrinsic energy by an amount of $\Delta\mu$ due to site-to-site interactions. The $^1/_2$ factor in (2.5) is necessary to avoid counting all pairwise interactions twice. Independent of the mechanism of these interactions, different microstates generally give different $\Delta\mu$ because a particular binding site will experience different microenvironments (spatial or chemical configurations) in different microstates. It is clear that without further simplification, partition function calculations will not be tractable because even for moderate-sized dendrimers, such as a fourth generation PAMAM dendrimer, the total number of microstates is astronomical. To get around this problem, we assume that $\Delta\mu$ is only a function of stoichiometry (i.e., k, l, h) but does not depend on the spatial configurations of the binding sites. This assumption is essentially the same as the mean-field approximation described by Borkovec and Koper.[9,15] Equation 2.1 now becomes

$$P = \sum_{k=0}^{k_0} \sum_{l=0}^{k} \sum_{h=0}^{h_0 - \gamma_M k} P(k,l,h) \tag{2.9}$$

where

$$P(k,l,h) = \sum_{m}^{\Omega(k,l,h)} \exp(-\beta_T \mu_m) = \Omega(k,l,h) \exp[-\beta_T \mu(k,l,h)] \tag{2.10}$$

$$\mu(k,l,h) = \mu^o(k,l,h) + \Delta\mu(k,l,h) \tag{2.11}$$

$$\Delta\mu(k,l,h) = \frac{1}{2}[(k-l)\Delta\mu_M(k,l,h) + l\Delta\mu_{MOH}(k,l,h) + h\Delta\mu_H(k,l,h)] \tag{2.12}$$

$P(k,l,h)$ is the contribution to the total partition function from all the microstates with a (k,l,h) stoichiometry, and the degeneracy factor $\Omega(k,l,h)$ is just the total number of such microstates:

$$\Omega(k,l,h) = \sum_{m}^{\Omega(k,l,h)} 1 = \binom{k_0}{k}\binom{k}{l}\binom{h_0 - \gamma_M k}{h} \tag{2.13}$$

The upper summation limits in (2.9) appear peculiar because k, l, h indexes are not completely independent of each other. In addition, (2.13) is affected similarly. The first binomial coefficient in (2.13) gives the number of ways one can fill k_0 sites with k metal ions. The third factor is also binomial since competitive binding leaves only $h_0 - \gamma_M k$ sites available for the proton. Finally, the second binomial factor gives the number of ways one can add to k occupied metal binding sites with l hydroxyl ions. The above accounting scheme implies that there is only one way to assemble k_0 metal binding sites using h_0 amine functional groups: an assumption obviously not valid if amine groups are completely free to choose which metal binding site they belong. Fortunately, due to steric constraints, amine groups that would bind to a common metal ion are likely to be located within the same shell and on the same dendrimer branch.[1,16] This local binding arrangement suggests that any correction factor to be applied to (2.13) will be small compared to the magnitude of $\Delta\mu$ or to errors from other assumptions such as the mean-field approximation. The correction factor is not needed if k is zero, such as in the case of dendrimer protonation in the absence of metal.

Since $P(k,l,h)$ is proportional to the probability of finding species $M_kOH_lH_hL$, we can write

$$\frac{[M_kOH_lH_hL]}{[L]} = \frac{P(k,l,h)}{P(0,0,0)} = P(k,l,h) \tag{2.14}$$

where $P(0,0,0) = 1$ because the free ligand L has been chosen as the zero-energy reference state. Expanding and rearranging (2.14), we have

$$\frac{[M_kOH_lH_hL]}{[M]^k[H]^{h-l}[L]} = \Omega(k,l,h)\beta_M{}^{(k-l)}\beta_{MOH}{}^{l}\beta_H{}^{h} \exp[-\beta_T \Delta\mu(k,l,h)] \tag{2.15}$$

Comparing (2.15) with (1.1), we conclude

$$\beta(k,l,h) = \Omega(k,l,h)\beta_M{}^{(k-l)}\beta_{MOH}{}^{l}\beta_H{}^{h} \exp[-\beta_T \Delta\mu(k,l,h)] \tag{2.16}$$

and it follows from (2.14)

$$P(k,l,h) = \beta(k,l,h)[M]^k[H]^{h-l} \tag{2.17}$$

Comparing (2.9) and (2.17) with (1.6), we obtain

$$P = \alpha_L{}^{-1} \tag{2.18}$$

The above results indicate that if the intrinsic binding constants β_M, β_{MOH}, and β_H, and free energy increase $\Delta\mu(k,l,h)$ can be calculated, then all the macroscopic binding parameters (such as $\bar{k}$, $\bar{l}$, and $\bar{h}$) can be predicted, as we have shown in section 1. However, unlike the results in section 1, the statistical method described in this section allows us to link apparent binding behaviors with the underlying chemical structures. For example, the apparent macroscopic stability constants $\beta(k,l,h)$ are now nicely linked to the intrinsic binding constants. Furthermore, $\Delta\mu(k,l,h)$ gives us a convenient entry point to study the nature of site-to-site interactions.

(3) Adsorption Isotherm Approach to Metal−Ligand Binding Equlibria. When implementing and optimizing computer algorithms for calculating the partition function, we noticed that as the number of binding sites (i.e., k_0, l_0, h_0) increases, the partition function is often dominated by a very few terms clustering near the $(\bar{k}, \bar{l}, \bar{h})$ index. In other words, most ligand molecules in an ensemble have a stoichiometry not far away from the average stoichiometry. This gives us a hint that the binding problem can now be thought of as an adsorption problem with the polymeric ligand acting as a surface with a large number of binding sites but the sites only belong to a very few distinctive types. For example, if $\bar{\nu}_H$ is the average number of vacancy sites per ligand molecule for H binding, then

$$\frac{\bar{h}}{\bar{\nu}_H} = \beta_H'[H] = B_H \tag{3.1}$$

where B_H is a symbol for notational simplicity and β_H' is a binding constant.[11] In the absence of site-to-site interactions, β_H' is exactly the same as β_H, the intrinsic binding constant used earlier. Equation 3.1 is just one form of the Langmuir adsorption isotherm, where β_H is independent of surface coverage, or $\bar{h}$. When site-to-site interactions are present, B_H' will depend on the coverage of all types of sites, and (3.1) will describe a Frumkin isotherm:[11]

$$\beta_H' = \beta_H \exp[-\beta_T \Delta\mu_H(\bar{k},\bar{l},\bar{h})] \tag{3.2}$$

where $\Delta\mu_H(\bar{k},\bar{l},\bar{h})$ should have the same functional form as $\Delta\mu_H(k,l,h)$ (in (2.12)). Similar treatments for the M and MOH binding sites result in

$$\frac{\bar{k}-\bar{l}}{\overline{\nu_M}} = \beta_M'[M] = B_M \tag{3.3}$$

$$\frac{\bar{l}}{\overline{\nu_M}} = \beta_{MOH}'[M][H]^{-1} = B_{MOH} \tag{3.4}$$

$$\beta_M' = \beta_M \exp[-\beta_T \Delta\mu_M(k,l,h)] \tag{3.5}$$

$$\beta_{MOH}' = \beta_{MOH} \exp[-\beta_T \Delta\mu_{MOH}(k,l,h)] \tag{3.6}$$

The numbers of vacancy sites for *H* and for *M* differ from each other:

$$\overline{\nu_H} = h_0 - \gamma_M \bar{k} - \bar{h} \tag{3.7}$$

$$\overline{\nu_M} = \frac{\overline{\nu_H}}{\gamma_M} \tag{3.8}$$

Recombining the above equations, we obtain

$$\overline{\nu_H} = h_0 \frac{1}{1 + B_H + B_M + B_{MOH}} \tag{3.9}$$

$$\bar{k} = k_0 \frac{B_M + B_{MOH}}{1 + B_H + B_M + B_{MOH}} \tag{3.10}$$

$$\bar{l} = k_0 \frac{B_{MOH}}{1 + B_H + B_M + B_{MOH}} \tag{3.11}$$

$$\bar{h} = h_0 \frac{B_H}{1 + B_H + B_M + B_{MOH}} \tag{3.12}$$

Like the statistical method, the isotherm method described in this section also allows calculation of all the macroscopic binding parameters ($\bar{k}$, $\bar{l}$, and $\bar{h}$) if the intrinsic binding constants β_M, β_{MOH}, and β_H, and free energy increase $\Delta\mu$ are given. In addition, $\Delta\mu$ still serves as an important link for investigating the nature of site-to-site interactions.

(4) Dendrimer Model for Calculating Electrostatic Interactions. Numerical implementation of both the statistical and the isotherm methods requires an explicit expression for $\Delta\mu$. Here, we will assume that electrostatic interaction energy is the sole source for $\Delta\mu$. To calculate $\Delta\mu$, we approximate a symmetric dendrimer with concentric shells, each shell bearing a charge specified by the binding stoichiometry and distributed evenly and continuously over the shell surface (Figure 1). The innermost core with radius r_C and dielectric constant ϵ_C is assumed to be inaccessible to solvent or electrolyte although

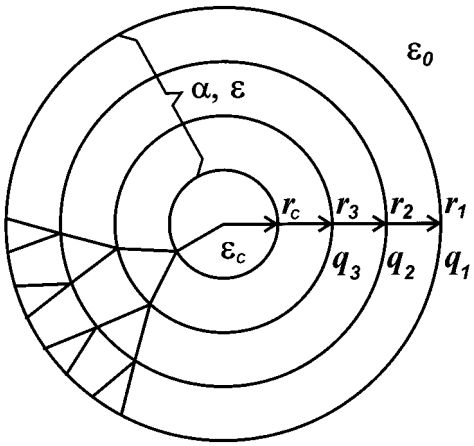

Figure 1. Dendrimer model for calculating site-to-site electrostatic interaction energy. Sites are grouped into concentric charged shells. As an example, only three charged shells and some branches are shown here.

setting r_C to zero does not influence the final result significantly.[17] Beyond this innermost core, the rest of the dendrimer structure occupies a region partially filled with an electrolyte solution having a dielectric constant of ϵ. The fraction of volume occupied by the electrolyte is assumed to be α. Outside the dendrimer molecule, we have a region where the electrolyte has a dielectric constant of ϵ_0 and extends to infinity.

A general procedure for solving spherically symmetric $\Delta\mu$ has been reported by Tanford, who used it to calculate the total interaction energy of a solid sphere uniformly filled with continuous charge.[12] We could have used this solid sphere as a dendrimer model; however, we selected the above shell model for several reasons. First, the shell model is easier to solve analytically than a solid sphere model, and sometimes even a single shell can give results equivalent to those for a solid sphere. Second, the shell model resembles the dendrimer structure more closely because charge is partially quantized as discrete shells. Finally, the shell model can be very flexible in coping with the need for testing various structural models: e.g., the number of shells can be adjusted conveniently by setting the charge on some shells to zero, and the binding constants for individual shells can be set independently.

According to the Debye−Hückel theory of electrolyte solutions, mobile ions around a fixed charge produce an electric potential that obeys the Poisson−Boltzmann equation:

$$\nabla^2 U(r) = \kappa^2 U(r) \tag{4.1}$$

where κ^{-1} is the Debye length beyond which most of the electric field from the fixed charge will be screened by the mobile ions.[18] Following Tanford's approach,[12] we applied (4.1) to our model shown in Figure 1 and arrived at an expression for the electric potential at the λth shell:

$$U_\lambda(\mathbf{q}) = \frac{f_0 e}{r_\lambda}(x_\lambda A_\lambda + y_\lambda B_\lambda) \qquad (1 \le \lambda \le \Lambda) \tag{4.2}$$

where e is the charge of an electron (positive value), r_λ is the radius of the λth shell, Λ is the total number of shells, and

$$\mathbf{q} = \{q_1, q_2, ..., q_\lambda, ..., q_\Lambda\} \tag{4.3}$$

is a Λ-dimensional vector denoting the overall charge configuration. f_0 is an empirical factor that is to be used to adjust the strength of site-to-site interactions. If a model is perfect, then

f_0 will be equal to 1. Other constants in (4.2) are unitless:

$$x_\lambda = x_1 + \sum_{\lambda'=2}^{\lambda} q_{\lambda'} B_{\lambda'}/R_{\lambda'} \qquad (\lambda \geq 2) \tag{4.4}$$

$$y_\lambda = y_1 - \sum_{\lambda'=2}^{\lambda} q_{\lambda'} A_{\lambda'}/R_{\lambda'} \qquad (\lambda \geq 2) \tag{4.5}$$

$$x_1 = \frac{Q_\Lambda(C_0B_1 - A_0D_1) - q_1A_0D_C}{C_C(C_0B_1 - A_0D_1) - D_C(C_0A_1 - A_0C_1)} \tag{4.6}$$

$$y_1 = \frac{q_1A_0C_C - Q_\Lambda(C_0A_1 - A_0C_1)}{C_C(C_0B_1 - A_0D_1) - D_C(C_0A_1 - A_0C_1)} \tag{4.7}$$

$$Q_\Lambda = D_C \sum_{\lambda=2}^{\Lambda} q_\lambda A_\lambda/R_\lambda - C_C \sum_{\lambda=2}^{\Lambda} q_\lambda B_\lambda/R_\lambda \tag{4.8}$$

$$R_\lambda = -2\epsilon\kappa r_\lambda \tag{4.9}$$

$$A_0 = \exp(-\kappa_0 r_1) \tag{4.10}$$

$$A_\lambda = \exp(-\kappa r_\lambda) \tag{4.11}$$

$$B_\lambda = \exp(\kappa r_\lambda) \tag{4.12}$$

$$C_0 = \epsilon_0(1 + \kappa_0 r_1)\exp(-\kappa_0 r_1) \tag{4.13}$$

$$C_\lambda = \epsilon(1 + \kappa r_\lambda)\exp(-\kappa r_\lambda) \tag{4.14}$$

$$D_\lambda = \epsilon(1 - \kappa r_\lambda)\exp(\kappa r_\lambda) \tag{4.15}$$

$$C_C = \epsilon(1 + \kappa r_C)\exp(-\kappa r_C) \tag{4.16}$$

$$D_C = \epsilon(1 - \kappa r_C)\exp(\kappa r_C) \tag{4.17}$$

$$\kappa_0 = \left(\frac{8\pi N_{AV} e^2}{\epsilon_0 k_B T \cdot 1000}\right)^{1/2} I^{1/2} \tag{4.18}$$

$$\kappa = \left(\frac{8\pi\alpha N_{AV} e^2}{\epsilon k_B T \cdot 1000}\right)^{1/2} I^{1/2} \tag{4.19}$$

where N_{AV} is Avogadro's number and I is the total ionic strength in moles per liter. If we bring a charge of $z_i e$ from infinity to shell λ, then the free energy increase due to pure electrostatic interactions will be

$$\Delta\mu_{i\lambda}(\mathbf{q}) = z_i e U_\lambda(\mathbf{q}) \qquad (i = \text{H, M, or MOH}) \tag{4.20}$$

Thus, in the above shell model, $\Delta\mu$ depends on a set of q_λ but not explicitly on $(k, l, h)_\lambda$. This expression is extremely useful for providing numeric results for $\Delta\mu$, which is required by the mean-field statistical method and the adsorption isotherm method.

It should be emphasized here that the equations presented in sections 2 and 3 are intended for a dendrimer model containing only a single shell. Nevertheless, it is straightforward to extend those equations to describe models containing multiple shells. For the statistical method, an extra summation index, or the shell index, is needed in the expression for the partition function, so (2.9) becomes

$$P = \sum_{\lambda=1}^{\Lambda} \sum_{(klh)_\lambda} \prod_{\lambda=1}^{\Lambda} P(k,l,h)_\lambda \tag{4.21}$$

Unfortunately, the two summation indexes cannot be separated because $\Delta\mu$ depends on the charge configuration of all the shells. As a result, when metal ion binding is included, the total computation time for a multishell model becomes impractical. We have partially alleviated this problem by skipping some of the Boltzmann factors in (4.21) if they are below a preset threshold. This approach will be called statistical method II, and its validity has been confirmed by comparing results to those when no skipping (method I) was used.[17]

For the isotherm method, (3.10), (3.11), and (3.12) still hold for each charged dendrimer shell. However, all the B factors are now functions of $\bar{\mathbf{q}}$ because $\Delta\mu$ is a function of $\bar{\mathbf{q}}$ according to (4.20). Combining these equations, we can express stoichiometric indexes $(\bar{k}, \bar{l}, \bar{h})_\lambda$ as functions of $\bar{\mathbf{q}}$ and obtain a charge balance equation for each shell:

$$\begin{aligned} f_\lambda(\bar{\mathbf{q}}) &= z_M(\overline{k_\lambda} - \overline{l_\lambda}) + z_{MOH}\overline{l_\lambda} + z_H\overline{h_\lambda} - \overline{q_\lambda} \\ &= z_M\overline{k_\lambda} - \overline{l_\lambda} + \overline{h_\lambda} - \overline{q_\lambda} = 0 \qquad (1 \leq \lambda \leq \Lambda) \end{aligned} \tag{4.22}$$

where z_M, z_{MOH}, and z_H are the charge of binding sites for M, MOH, and H, respectively; and, as mentioned previously, we have assumed in this work

$$z_{MOH} = z_M - 1 \qquad z_H = 1 \tag{4.23}$$

Equation 4.22 represents Λ coupled nonlinear equations; thus, Λ unknowns, i.e., $\bar{\mathbf{q}}$, can be solved if the intrinsic binding constants β_M, β_{MOH}, β_H, and $\Delta\mu$ are given. General methods for solving coupled nonlinear equations do not always lead to a complete set of converging roots.[19] Fortunately, all $f_\lambda(\bar{\mathbf{q}})$ decreases monotonically as any $\overline{q_\lambda}$ increases, and this makes it easy for us to devise an efficient computer algorithm that searches in a Λ-dimension $\bar{\mathbf{q}}$ space. Solutions to $\bar{\mathbf{q}}$ are found when all $f_\lambda(\bar{\mathbf{q}})$ reach zero.

(5) Numerical Results. *Comparison of the Statistical and Isotherm Methods.* Computation time based on the isotherm method is shorter than those based on the statistical method II (Table 1), but the former is perhaps more crude because it only deals with "an average dendrimer molecule" with averaged proton and metal binding numbers. To find out how much error this approximation will introduce, we compared the simulated binding curves calculated using the above two computational methods. The agreement is excellent if only proton binding is considered.[17] However, when metal binding is also included, the metal binding constants in the isotherm method have to be decreased slightly (about 0.5 logarithmic unit) in order to match the curve from the statistical method.

Characteristics of a Multishell Dendrimer Model. We have seen that, in the statistical approach, a binding site is an averaged site because it experiences only a mean field. The isotherm approach goes a step further, using only a representative molecule with averaged binding numbers. These underpinning assumptions make us wonder if a multishell model is really necessary *when sites of the same kind in different shells have the same intrinsic binding constant*. A direct way to answer this question is to compare the results with a single-shell model

TABLE 1: Comparison of Computation Time (s) for Three Numeric Algorithms[a]

shell configurations	statistical method I	statistical method II	isotherm method
1 shell: H binding only	0.11	0.060	<0.001
2 shells: H binding only	2.7	0.50	0.050
5 shells: H binding only	10 600	753	44
1 shell: H and M binding	26	5.8	0.22
2 shells: H and M binding	134 000	1750	0.39
5 shells: H and M binding	—	—	354

[a] Note: (a) In statistical method I, no terms in a partition function are skipped. (b) In method II, some terms below a preset threshold are predicted and skipped. (c) The shell configurations are modeled with a NH_2-terminated PAMAM dendrimer in mind: a 1-shell model includes only 64 H-binding sites and all the inner shells are ignored. A 2-shell model has a (64, 32) configuration, and a 5-shell model has (64, 32, 16, 8, 4) binding sites. When competitive M binding is included in a model, the amount of M is set to be 30% of its maximum binding number. (d) All computation is carried out using a custom-written program on a desktop computer (Dell, Dimension 4100, Pentium III/733 MHz). The times listed are the times for completing calculation of a 50-point pH titration curve. These results represent typical ones since the exact times will change when other parameters (such as binding constants, solution concentrations, and ionic strength) change. (e) All numbers have a unit of seconds. A "—" entry means that the time is expected to be very long, and it has not been tested.

where the total number of binding sites is the same as the one in a multishell model. This single-shell model removes some structural details about the dendrimer so binding properties may be viewed as shell-averaged ones. In addition, the diameter of the single shell no longer has a clear physical meaning. Figure 2 shows that if all shells have the same set of intrinsic binding constants for M, MOH, and H, then a single-shell model gives nearly the same results as those from a multishell model.[20]

The above result implies that, in some cases, the form of the interaction energy may be independent of the total shell number, although this is not obvious when examining the complicated analytical expression for $\Delta\mu$ shown in (4.20). Substituting (2.12), (2.16), (2.17), and (4.20) into (4.21), we can show that indeed the partition function for a multishell model can be recast into

$$P = \sum_{KLH} \Omega(K,L,H)\beta_{\mathrm{M}}{}^{K-L}\beta_{\mathrm{MOH}}{}^{L}\beta_{\mathrm{H}}{}^{H}10^{-\Delta W}[\mathrm{M}]^{K}[\mathrm{H}]^{H-L} \tag{5.1}$$

where (K, L, H) specifies the overall stoichiometry, $\Omega(K,L,H)$ is the total number of microstates contained under this stoichiometry, and ΔW is a unitless total interaction energy:

$$\Delta W = \frac{1}{2}\sum_{\lambda=1}^{\Lambda}\delta_\lambda q_\lambda \tag{5.2}$$

$$\delta_\lambda = \frac{f_0 e^2}{k_{\mathrm{B}}T\ln(10)}\frac{(x_\lambda A_\lambda + y_\lambda B_\lambda)}{r_\lambda} \tag{5.3}$$

δ_λ can be thought of as a unitless $\Delta\mu$ per unit bound charge at shell λ. A necessary, although not sufficient, condition for (5.1) to be reduced to the single-shell form is that ΔW depends just on the overall stoichiometry, but not on the stoichiometry of a specific shell, i.e., (k, l, h). In fact, we find (see Figure 3B), through direct simulation, that ΔW varies quadratically with respect to the total charge Q:

$$2\Delta W = \bar{w}Q^2 = \bar{\delta}Q \tag{5.4}$$

where $\bar{w}$ is a constant. In other words, the average interaction energy per unit bound charge $\bar{\delta}$ is a linear function of Q with a slope of $\bar{w}$:

$$\delta = \frac{2\Delta W}{Q} = \frac{\sum_{\lambda=1}^{\Lambda}\delta_\lambda q_\lambda}{\sum_{\lambda=1}^{\Lambda} q_\lambda} = \bar{w}Q \tag{5.5}$$

so $\bar{\delta}$ is just a charge-averaged δ_λ. The linearity of $\bar{\delta}$ with respect to Q implies that each δ_λ is also a linear function of Q

$$\delta_\lambda = w_\lambda Q \tag{5.6}$$

Substituting (5.6) into (5.5), it can be shown that $\bar{w}$ is a charge-averaged variable as well:

$$\bar{w} = \frac{2\Delta W}{Q^2} = \frac{\sum_{\lambda=1}^{\Lambda} w_\lambda q_\lambda}{\sum_{\lambda=1}^{\Lambda} q_\lambda} \tag{5.7}$$

$\bar{w}$ is proportional to the strength of site-to-site interactions, and it is characteristic of the dendrimer geometry.

Comparison with the Ising Model. Although equivalent to a single-shell model under certain conditions, the multishell model

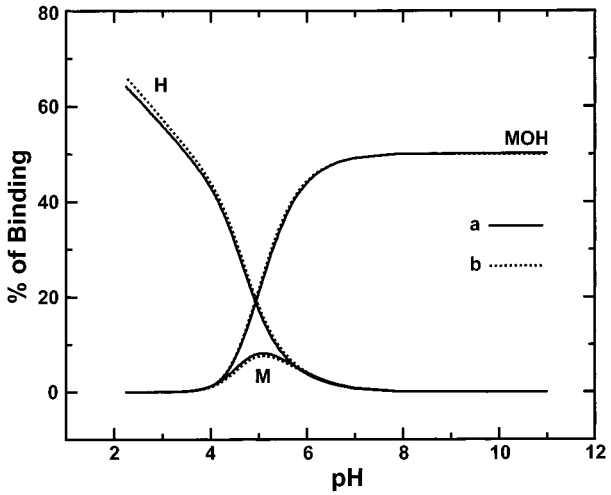

Figure 2. Equivalence of (a) 4-shell (solid line) and (b) 1-shell (dotted line) models for an abstract OH-terminated PAMAM dendrimer: average binding numbers of three types of binding sites (M, MOH, and H), expressed as a percentage of the maximum binding numbers, as a function of pH. The geometric structure of the 4-shell model is assumed to be an outer shell of OH groups with zero charge ($q_1 = 0$) and a diameter of 4.5 nm and four shells of binding spheres with a configuration of 3.6 nm (32), 2.9 nm (16), 2.2 nm (8), and 1.5 nm (4) with the numbers in parentheses denoting the maximum number of binding sites in each shell.[20] The structure of the generic 1-shell model includes two shells: an outer shell of OH groups that do not bind and an inner shell with a maximum binding number of 60 (the sum of the 4-shell model). Their effective diameters are slightly smaller than those used in the 4-shell model, corresponding to f_0 of 1.034 in eq 5.3. In both models, the binding constants for M and H are both set to 7.0 (10-based logarithm), the dielectric constant of the outer medium is 80.36, the dielectric constant of the dendrimer is 60, the fractional void volume is 1.0, the ionic strength is 0.01 M, the dendrimer concentration is 0.2 mM, and $z_{\mathrm{M}} = \gamma_{\mathrm{M}} = 2$. The amount of M present is set to be 50% of its stoichiometric amount; thus, the maximum binding for M is leveled at 50% in this graph.

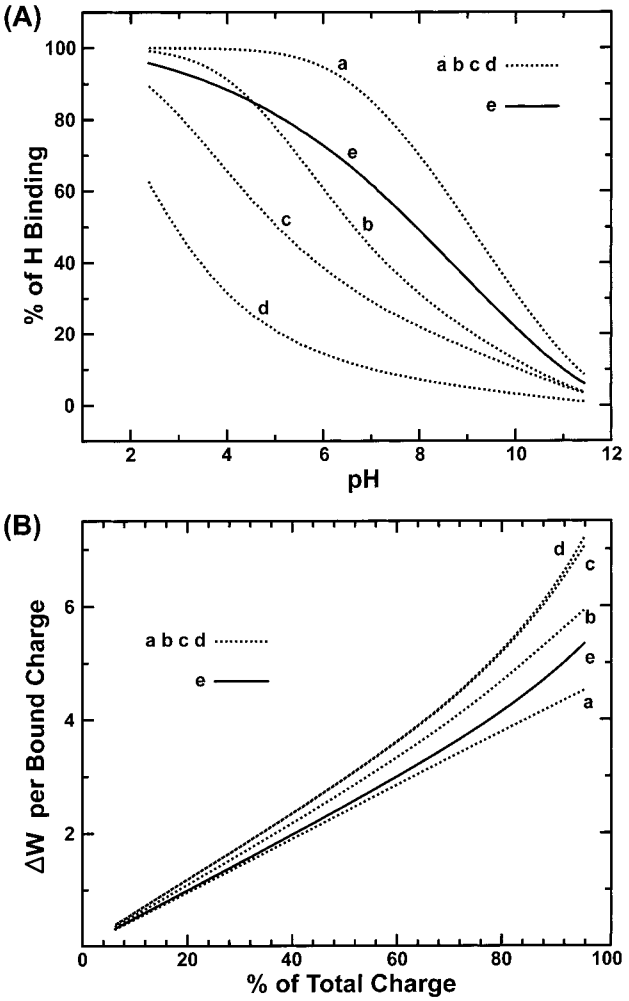

Figure 3. (A) H binding curves of a 4-shell model for an abstract PPI dendrimer: average H binding number, expressed as percentage of the maximum binding number, as a function of pH for the (a) first-shell (16 sites), (b) second-shell (8 sites), (c) third-shell (4 sites), (b) fourth-shell (2 sites), and (e) sum of all shells. The geometric structure of the 4-shell model is assumed to be an outer shell of NH_2 groups with a diameter of 1.9 nm and three shells of tertiary amines with diameters of 1.4, 0.9, and 0.75 nm, respectively. The log-binding constants for each shell have been chosen to be close to the values used by B&K: 10.7 for the primary amines, 10.35 for the tertiary amines, and 9.8 for the inner two nitrogens.[8] Other parameters are similar to those used in Figure 2, except the dendrimer concentration is 1.0 mM and f_0 is set to 0.815, corresponding to an effective interaction parameter $\bar{w}$ of 0.05. This choice seems to highlight the difference between shells, and other choices of $\bar{w}$ tend to give shell-level binding curves having the same shape as the overall binding curve. (B) Average interaction energy per bound charge ($\bar{\delta}$) as a function of the total charge (Q). The linearity, as described in (5.5), is maintained only when Q is 75% below its maximum value. The legends for each curve are the same as those in (A).

is still useful to simulate cases where different shells have different sets of binding constants. In addition, it can be illustrated here that a multishell model is also useful for testing an important conclusion from B&K's Ising model: that is, odd-numbered dendrimer shells are protonated at a different pH than the even-numbered shells.[7,8] Experimentally, this is seen as a titration curve with a plateau region flanked by two transition steps corresponding to proton binding at the above two groups of shells. It is important to point out that, in the Ising model, the intrinsic proton binding constants pK_H at all sites do not differ appreciably from each other, so the two steps are entirely due to electrostatic interactions between neighboring shells. However, using our shell model, we have failed to duplicate this feature after trying many combinations of structural parameters, including adjusting the interaction energy to highlight the difference between shell-level binding curves. Generally, we see sites at inner shells experiencing more electrostatic repulsion than those in outer shells; therefore, inner-shell binding is weaker than that at outer shells at any given pH but no odd−even behavior characteristic of an Ising model is observed (Figure 3A).

Many factors might be responsible for this difference in models but we feel that that only two related factors are important. First, the mean-field approximation used in our shell model is expected to fail when site-to-site interactions are strong.[10] The failure is the result of ignoring *site-to-site correlation*. Mean-field approximation says that the total interaction energy depends only on the number of sites occupied but not on their spatial distribution. In a sense, this approximation and the assumption of a uniformly distributed charge we used in deriving (4.2) are consistent and compatible with one another: both ignore the spatial structure of charge within a dendrimer shell. We want to emphasize here that we have also used a continuous charge approximation in (4.2), but it should be distinguished from the uniform charge assumption. The continuous charge approximation consistently leads to overestimation of the total interaction energy, especially when the binding number is small.[17] However, as our results (Figure 3) indicate, the absolute strength of interaction energy alters little the overall characteristics of the binding curve: a curve that changes monotonically as a function of pH without a middle plateau region. In contrast, site-to-site correlation is the highlight of B&K's Ising model. For example, imagine six binding sites on a linear ring, and assume that only nearest-neighbor interactions are significant. Obviously, three sites can be filled without incurring much free energy penalty because they can be arranged with zero nearest-neighbor. This configuration will be observed in reality with a high probability (large Boltzmann weighting) whereas others are less likely. However, when the remaining sites are filled, there will be a steep increase in the overall interaction energy (two to six nearest neighbors will be formed). Thus, if interactions are strong, the second group of sites will appear to protonate at a pH well separated from the first group of three sites. This is exactly the even−odd behavior discussed earlier.

The second factor responsible for the difference in models is related to the nearest-neighbor approximation commonly used in Ising models. B&K's Ising model counts nearest neighbors using a topological tree so interactions between sites located on two different branches are completely ignored.[7] This is effectively the same as saying that intrashell charge interactions are absent. As a consequence, shell-to-shell interactions appear more prominent than they actually are. An obvious remedy is to include next-nearest-neighbor interactions. However, this will probably require more computational power, thus further restricting the scope of the Ising model, especially when metal binding is included.

Simulation of pH Binding Curves. We now focus our attention on the effects of one variable, namely, the strength of site-to-site interactions, on pH binding curves. The effects of other variables, such as binding constants, will be discussed in a subsequent paper.

Interaction energy can be changed by many variables, including the dendrimer geometric structure (shell radii), ionic strength, and dielectric constants. To express our results more generally, the strength of interactions is adjusted by changing

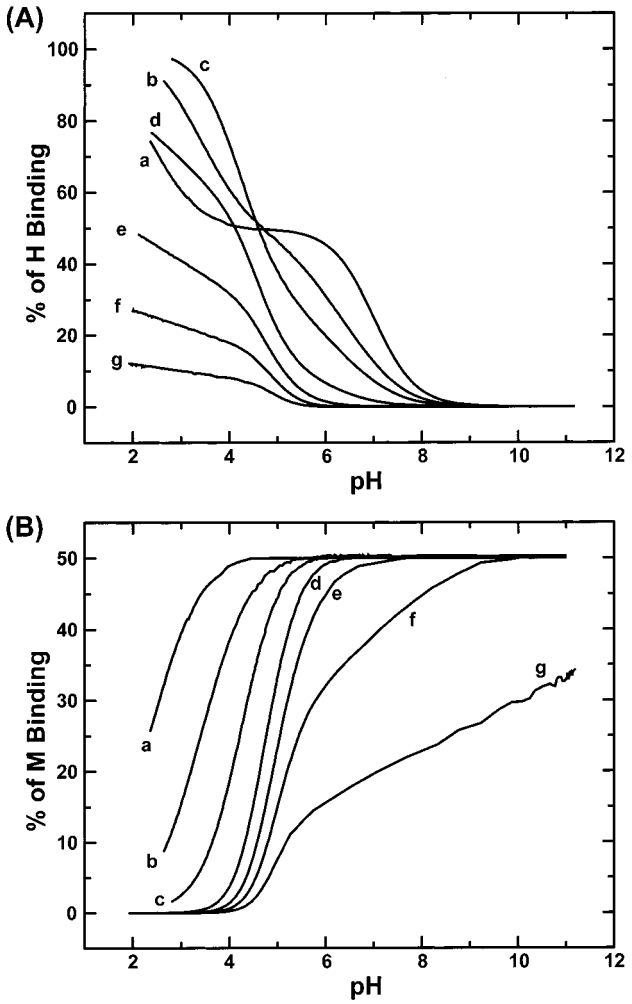

Figure 4. Progression of binding curves as the strength of site-to-site interactions increases: by adjusting f_0, $\bar{w}$ is set to (a) 0.00, (b) 0.01, (c) 0.02, (d) 0.05, (e) 0.1, (f) 0.2, and (g) 0.5. An abstract OH-terminated PAMAM dendrimer, which has the same set of geometric parameters as the model used in Figure 2, is used here. For clarity, the binding numbers for H are shown in a separate graph (A), and the binding numbers for M and MOH are combined into a single number in (B).

the magnitude of $\bar{w}$ in eq 5.4. As $\bar{w}$ increases, it becomes easier to deprotonate a dendrimer so the apparent transition point at half-protonation for H binding moves toward the low pH end (Figure 4A). Meanwhile, competitive binding between M and H shows an interesting trend. If we assume that both have the same intrinsic binding constants, then M binding seems to be less competitive as the strength of interactions increases. Thus, the transition pH, at which M reaches the half-saturation point, systematically moves toward the high pH end (Figure 4B). This feature is expected for multivalence metal ions. Consider the case where $z_M = \gamma_M > 1$: if all sites are occupied by M, then the total number of pairwise interactions experienced with a single test charge will be reduced by a factor of z_M compared to the case when all sites are occupied by protons. However, from Coulomb's law, the strength of each pairwise interactions should grow roughly by a factor of z_M^2. Thus, there is a free energy penalty when replacing z_M protons with one metal ion. Another interesting feature in Figure 4 is that when site-to-site interactions are extremely strong, the binding numbers for both M and H cannot reach their saturation limits within a reasonable but wide window (pH 2 to pH 12).

Summary

In this study, we have used a shell model to study proton and metal ion binding equilibria with dendrimers. Numeric results based on this shell model are obtained using two computational methods: a statistical method and an isotherm method. Both methods give similar results, but the isotherm method requires less computation time. Therefore, we anticipate that the latter will be adopted more readily, especially by experimental chemists who wish to obtain results quickly using only desktop computers.

Binding of charged probe ions to dendrimers is difficult to study using conventional or phenomenological methods because the connection between macroscopic binding constants and microscopic chemical structures is indirect. In contrast, methods presented here only contain a set of intrinsic binding constants for a few distinctive binding sites. These intrinsic binding constants are more useful in characterizing the chemical structure of a binding site than apparent macroscopic binding constants. We will show in a subsequent paper how to extract binding constants from experimental data.

Beyond site-level parameters, one often wishes to model the spatial configuration of a charged polymer. In fact, such information has been routinely incorporated in models for proteins.[10,21−23] Compared to the methods used by the researchers working in the field of protein folding and ionization, the methods reported here are much less sophisticated. Nevertheless, we did make a modest attempt to predict the spatial distribution of bound charge by approximating a dendrimer as discrete charged shells. For example, our results show that binding at an inner shell is weaker than that at an outer shell even if the intrinsic binding constants for all the shells are identical. However, the reliability of such predictions is still uncertain because they depend on specific choice of structure models. The disagreement between our results and those predicted with the Ising model of Borkovec and Koper is a good example of the above point. Our methods also require the use of mean-field approximation, which tends to give large errors when site-to-site interactions are strong. More accurate results will be obtained if binding sites are treated as discrete charges and site-to-site correlation is explicitly included.[10,21] However, doing so probably will not yield an analytical solution for the electric potential, and the Poisson−Boltzmann equation will have to be solved numerically.[24]

Acknowledgment. We gratefully acknowledge the Office of Naval Research for full support of this work.

Supporting Information Available: Text and figures on the following topics: (a) comparison between statistical and isotherm methods, (b) influence of core diameters on simulation results, and (c) evaluation of errors due to continuous charge approximation. This material is available free via the Internet at http://pubs.acs.org.

References and Notes

(1) Zhao, M.; Sun, L.; Crooks, R. M. *J. Am. Chem. Soc.* **1998**, *120*, 4877−4878. Preparation of Cu Nanoclusters within Dendrimer Templates.

(2) Zhao, M.; Crooks, R. M. *Angew. Chem., Int. Ed. Engl.* **1999**, *38*, 364−366. Homogeneous Hydrogenation Catalysis using Monodisperse, Dendrimer-Encapsulated Pd and Pt Nanoparticles.

(3) Grohn, F.; Bauer, B. J.; Akpalu, Y. A.; Jackson, C. L.; Amis, E. J. *Macromolecules* **2000**, *33*, 6042−6050. Dendrimer Templates for the Formation of Gold Nanoclusters.

(4) Sideratou, Z.; Tsiourvas, D.; Paleos, C. M. *Langmuir* **2000**, *16*, 1766−1769. Quaternized Poly(propylene imine) Dendrimers as Novel pH-Sensitive Controlled-Release Systems.

(5) Kukowska-Latallo, J. F.; Bielinska, A. U.; Johnson, J.; Spindler, R.; Tomalia, D. A.; Baker, J., Jr. *Proc. Natl. Acad. Sci. U.S.A.* **1996**, *93*, 4897−4902. Efficient Transfer of Genetic Material into Mammalian Cells using Starburst Polyamidoamine Dendrimers.

(6) Zhang, H.; Dubin, P. L.; Ray, J.; Manning, G. S.; Moorefield, C. N.; Newkome, G. R. *J. Phys. Chem. B* **1999**, *103*, 2347−2354. Interaction of a Polycation with Small Oppositely Charged Dendrimers.

(7) Borkovec, M.; Koper, G. J. M. *Macromolecules* **1997**, *30*, 2151−2158. Proton Binding Characteristics of Branched Polyelectrolytes.

(8) Koper, G. J. M.; van Genderen, M. H. P.; Elissen-Roman, C.; Baars, M. W. P. L.; Meijer, E. W.; Borkovec, M. *J. Am. Chem. Soc.* **1997**, *119*, 6512−6521. Protonation Mechanism of Poly(propylene imine) Dendrimers and Some Associated Oligo Amines.

(9) Borkovec, M.; Koper, G. J. M. *J. Phys. Chem.* **1994**, *98*, 6038−6045. Ising Models of Polyprotic Acids and Bases.

(10) Bashford, D.; Karplus, M. *J. Phys. Chem.* **1991**, *95*, 9556−9561. Multiple-Site Titration Curves of Proteins: An Analysis of Exact and Approximate Methods for Their Calculation.

(11) Bard, A. J.; Faulkner, L. R. *Electrochemical Methods, Fundamentals and Applications*; Wiley: New York, 1980.

(12) Tanford, C. *Physical Chemistry of Macromolecules*; Wiley: New York, 1961.

(13) Martell, A. E.; Motekaitis, R. J. *Determination and Use of Stability Constants*; VCH Publishers: New York, 1992.

(14) McQuarrie, D. *Statistical Mechanics*; Harper and Row: New York, 1976.

(15) Baxter, R. J. *Exactly Solved Models in Statistical Mechanics*; Academic Press: New York, 1982.

(16) Bosman, A. W.; Schenning, A. P. H. J.; Janssen, R. A. J.; Meijer, E. W. *Chem. Ber./Recueil* **1997**, *130*, 725−728. Well-Defined Metallodendrimers by Site-Specific Complexation.

(17) See data in the Supporting Information.

(18) Probstein, R. F. *Physicochemical Hydrodynamics: An Introduction*; Butterworth: Boston, 1989.

(19) Press: W. H.; Flannery, B. P.; Teukolsky, S. A.; Vetterling, W. T. *Numerical Receipes in C*; Cambridge University Press: Cambridge, 1988; Chapter 9.

(20) Structural parameters of dendrimers used here are determined by either size-exclusion chromatography or small-angle neutron scattering: see, e.g.: Crooks, R. M.; Zhao, M.; Sun, L.; Chechik, V.; Yeung, L. K. *Acc. Chem. Res.* **2000**, *34*, 181−190.

(21) Tanford, C.; Roxby, R. *Biochemistry* **1972**, *11*, 2192−2198. Interpretation of Protein Titration Curves. Application to Lysozyme.

(22) Honig, B.; Nicholls, A. *Science* **1995**, *268*, 1144−1149. Classical Electrostatic in Biology and Chemistry.

(23) Beroza, P.; Case, D. A. *J. Phys. Chem.* **1996**, *100*, 20156−20163. Including Side Chain Flexibility in Continuum Electrostatic Calculations of Protein Titration.

(24) Rajasekaran, E.; Jayaram, B.; Honig, B. *J. Am. Chem. Soc.* **1994**, *116*, 8238−8240. Electrostatic Interactions in Aliphatic Dicarboxylic Acids: A Computational Route to the Determination of pK_a Shifts.